A portable microevaporator for low temperature single atom studies by scanning tunneling and dynamic force microscopy

H.-P. Rust, T. König, G. H. Simon, M. Nowicki,[a] V. Simic-Milosevic, G. Thielsch, M. Heyde,[b] and H.-J. Freund
Fritz-Haber-Institut der Max-Planck-Gesellschaft, Faradayweg 4-6, D-14195 Berlin, Germany

(Received 2 September 2009; accepted 2 November 2009; published online 30 November 2009)

Here, we present a microevaporator setup for single adatom deposition at low temperature, which is a prerequisite for most single atom studies with scanning probe techniques. The construction of the microevaporator is based on the tungsten filament of a modified halogen lamp, covered with the required adsorbate. Very stable evaporation conditions were obtained, which were controlled by the filament current. The installation of this microevaporator on a manipulator enabled its transportation directly to the sample at the microscope kept at 5 K. In this way, the controlled deposition of Li onto Ag(100), Li, Pd, and Au onto MgO/Ag(001) as well as Au onto alumina/NiAl(110) at low temperature has been performed. The obtained images recorded after the deposition show the presence of single Li/Au atoms on the sample surfaces as a prove for successful dispersion of single atoms onto the sample surface using this technique. © *2009 American Institute of Physics.* [doi:10.1063/1.3266971]

I. INTRODUCTION

Surface science and miniaturization processes in many technological fields aim to understand processes at the atomic level. Surface sensitive methods providing information at the atomic level are scanning tunneling microscopy and dynamic force microscopy.[1–7] Both techniques have proven their possibility to map and manipulate single atoms in a controlled manner.[6,8] However, a prerequisite is high dispersion single atoms of a defined species. This reduces the number of commonly used preparation methods matching these needs. The deposition of adspecies from Knudsen cells or alkali metal dispenser comes with a couple of drawbacks. Beside the fact that operating these evaporator types at low coverage parameters is often difficult, they can hardly be operated in liquid helium temperature environments. Their operation conditions at high currents couple to much heat into the low temperature environment. Beside these technical issues, adspecies deposition at room temperature often leads to clustering, making single adatoms scarce on the surface. The important points for single adatom deposition are an efficiently cooled sample during the deposition process and a limited heat transfer from an evaporator into the cooling environment. Since heat capacities at liquid helium temperature are quite small, small powers and evaporation times are desired to keep the temperature increase as low as possible. Here, we have used a modified halogen lamp mounted onto a sample carrier. This microevaporator can be gripped by the manipulator and transferred to the 5 K area where the sample is located. The direct access to the cold sample is only possible via a manipulator from above. The electrical connections to the microevaporator are made via the manipulator.

II. EXPERIMENTAL SETUP

In our experimental setup, operating in ultrahigh vacuum (UHV), the sample, the microscope, and surrounding flanges are kept at 5 K. The microscope allows the simultaneous acquisition of the tunneling current in combination with frequency modulation dynamic force microscopy (FM-DFM) detection. Details of the microscope can be found in Refs. 9 and 10.

The assembly of the portable microevaporator is very simple. In Fig. 1(a), a schematic drawing of the portable low temperature microevaporator is provided and of its evaporation position when transferred into the low temperature microscope stage Fig. 1(b). There are two pairs of metal bars (2) fitted to the base sapphire plate (1) (dimension of the sapphire 25×20 mm^2) by three screws through the sapphire. These metal bar pairs enable gripping with the manipulator. One of the pairs is used as an electrode for the tungsten filament (4), which is part of a standard halogen lamp (3) where the glass bulb has been removed. The other contact to the tungsten filament is established by a contact wire (5). Furthermore, it has a very small mass giving rise to the name microevaporator. Due to its small mass, only a power of 700 mW for several seconds is necessary to start annealing the filament. The residual of the halogen lamp with the filament is mounted off axis and has an angle of about 15° with respect to the sample to enhance the adsorption rate on the surface. A geometric arrangement of evaporator and sample is shown in Fig. 1(b).

We have established an *ex situ* and an *in situ* loading mode for the microevaporator. In the *ex situ* mode, we have introduced a gold or palladium (Au/Pd) wire into the tung-

[a]Present address: Institute of Experimental Physics, University of Wrocław, pl. Maxa Borna 9, 50-204 Wrocław, Poland.
[b]Electronic mail: heyde@fhi-berlin.mpg.de.

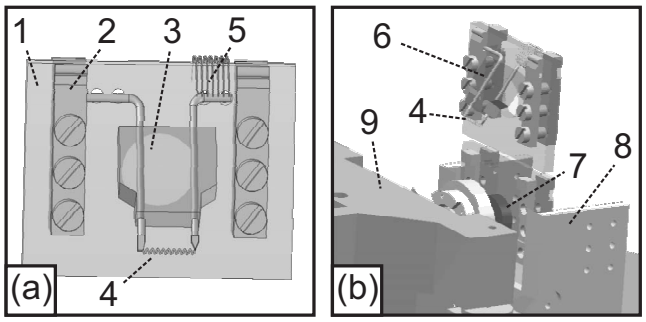

FIG. 1. (a) Schematic drawing of the portable low temperature microevaporator for single atom deposition: (1) sapphire plate (dimension 25 $\times 20$ mm^2), (2) molybdenum bars, (3) halogen lamp with glass bulb removed, (4) filament, and (5) electrical contact. (b) Overview of the microscope stage with the evaporator at the evaporation position above the sample. The manipulator holding the evaporator is not shown. (4) Filament, (6) evaporator, (7) sample, (8) sample-stage, and (9) microscope slider.

sten filament of the microevaporator outside the UHV chamber. Then, the microevaporator is transferred into the chamber via a load lock. The tungsten filament is heated until the Au/Pd wire melts and wets the filament (about 700 mW).

In the *in situ* loading mode, the clean tungsten filament is loaded inside the UHV chamber. The microevaporator is located in front of an alkali dispenser. The alkali dispenser is heated such that it evaporates the desired material. In our experiments, we used a Li dispenser.[11] The Li will adsorb on the tungsten filament of the microevaporator and the load depends mainly on the power applied to the dispenser and time. For alkali metals, we believe that, at annealing temperatures, the full amount of the material previously adsorbed on the tungsten filament will be evaporated. Therefore, the coverage depends for alkali metals strongly on the loading parameters of the tungsten filament. However, the *in situ* loading mode can be applied to any *in situ* source available and is not limited to alkali dispensers.

Before starting the evaporation process, it is important to move the microscope slider (9) in Fig. 1(b), carrying the scanning tunneling microscope (STM)/FM-DFM sensor as far as possible away from the sample to avoid its contamination by the evaporating material. To prevent a deposition onto tip and scanner piezos, an additional shield can be mounted either to the microevaporator or the microscope stage (shield not shown in Fig. 1).

The deposition of the desired material is achieved by the following procedure. The loaded microevaporator is transferred via the manipulator into the low temperature area of the microscope. The pressure in the UHV chamber, the sample temperature, and the temperature of the microscope stage during the process are presented in Fig. 2(a). At first, the valve separating the room temperature area of the UHV chamber and the so-called pendulum [Fig. 2(b)], which is situated in an exchange gas canister, is opened. The base pressure in the room temperature area is in the lower 10^{-10} mbar regime [upper graph, Fig. 2(a)], while the base pressure at the microscope stage is supposed to be in the 10^{-12} mbar regime or even better which is supported by clean sample surfaces for several weeks without contaminations present. Due to the movement of the valve, the pressure

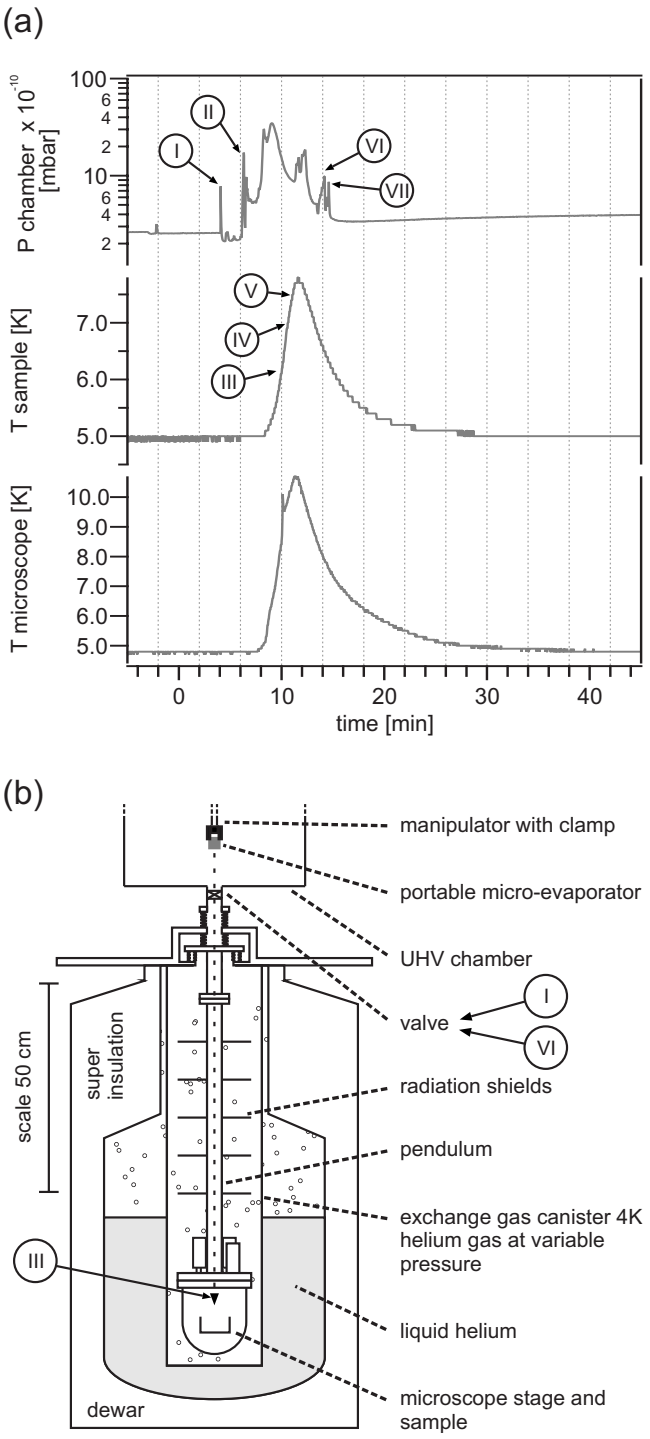

FIG. 2. (a) Pressure in the room temperature area of the UHV chamber, temperature of the sample in the microscope stage, and temperature of the microscope stage during the evaporation procedure with respect to time (see text): (I) valve to pendel is opened, (II) starting the transfer of the microevaporator to the cold microscope stage, (III) evaporator at evaporation position, (IV) start evaporation, (V) stop evaporation and retract manipulator, (VI) valve is closed, and (VII) movement of the manipulator is stopped. (b) Schematic of the UHV setup including the bath cryostat.

in the room temperature area increases, as indicated by number I in Fig. 2(a) upper graph. Next, the manipulator starts moving. This leads to a pressure peak indicated by number II. However, due to the high pumping rate of the cryostat, no contaminations can reach the sample. The microevaporator is transferred to the exact position slightly above the sample

(number III). The alignment of the microevaporator with respect to the sample has to be done carefully. Then, the evaporation process starts and the Li/Au/Pd is evaporated at a filament power of 800 mW (number IV). After the desired evaporation time, the filament current is switched off (number V) and the manipulator moves directly upwards into the room temperature area. Finally, the valve is closed (number VI) and the manipulator stopped (number VII).

III. RESULTS AND DISCUSSION

The coverage depends on time and power, resulting from voltage and current applied to the filament. Furthermore, the heat coupled into the microscope is determined by these parameters. For an evaporation time of 20 s at 800 mW, the temperature of the microscope stage increases to 10.7 K, while the sample temperature increases to only 7.8 K. The microscope compartment is heated stronger through the manipulator making contact with the pendulum. The tip approach can be started directly after the deposition. However, the temperature during the evaporation process, as well as the cool down time, depends on the liquid helium level in the bath cryostat and the helium gas pressure in the exchange gas canister.[12] Depending on the approach parameters, the tip is after 20 min in the tunneling regime. This is also the time needed to cool down microscope stage and sample to base temperature [note: the zero time of the abscissa in Fig. 2(a) has been arbitrarily chosen]. This ensures a small thermal drift and stable operation conditions. Overall, the time for the evaporation process until scanning the surface does not take more than 30 min.

The above presented deposition method has been employed in the sample preparation for STM and FM-DFM studies. With the presented procedure, highly reproducible deposition rates have been obtained [see Figs. 3(a)–3(c)]. The images show different coverages of Au on alumnia/NiAl(110) generated by different evaporations times at a power of 800 mW. For the surface preparation shown in Figs. 3(a)–3(c), evaporation times of 10, 20, and 30 s have been chosen, respectively. The corresponding coverages are 0.03 ± 0.01, 0.07 ± 0.01, and 0.09 ± 0.01 atoms/nm^2. Figure 3(d) shows the coverage dependence with respect to evaporation time at a filament power of 800 mW. In this low coverage regime necessary for single atom investigations, the coverage depends linear on evaporation time for a constant filament power. Evaporation times above 30 s will result in clustering and are not recommended for single adatom studies.

FM-DFM investigations underline the need for low temperature deposition of metal atoms. FM-DFM images of highly dispersed Au atoms are shown in Fig. 4. In general, they are only obtained at force interactions much weaker than for the typical values necessary to resolve the alumina film. These measurements show that Au atoms bind weakly to alumnia and may therefore cluster when deposited at room temperature, making single atom studies impossible. Such a case has been studied for Li on freshly prepared Ag(001) and is presented in Figs. 5(a)–5(d).

In Figs. 5(a) and 5(b), lithium has been deposited at room temperature directly onto Ag(001) from a SAES dispenser. Figures 5(c) and 5(d) show Li deposited onto Ag(001) at 5 K using the microevaporator,[13] which has been loaded by the above described *in situ* loading mode. The

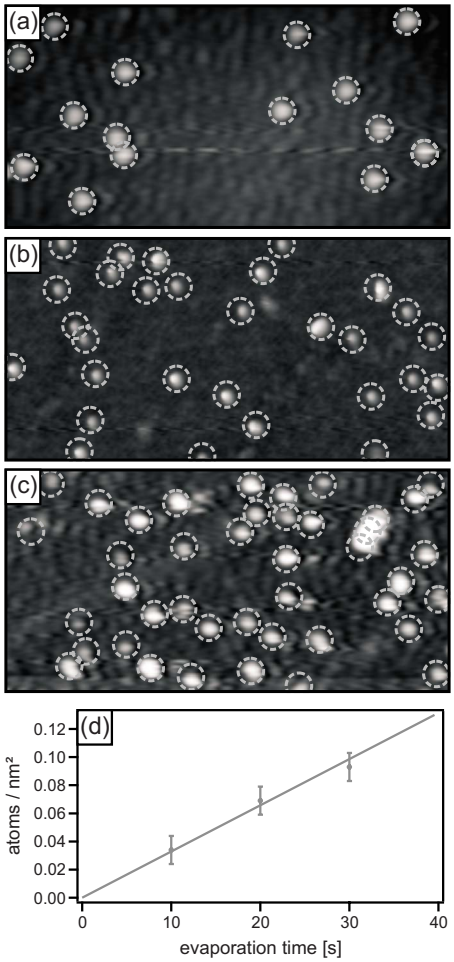

FIG. 3. (Color online) [(a)–(c)] STM images of Au deposited on alumina/NiAl(110) for different evaporation times (a) 10 s, (b) 20 s, and (c) 30 s at 800 mW. Image (a) shows a coverage of 0.03 atoms/nm^2, (b) 0.07 atoms/nm^2, and (c) 0.09 atoms/nm^2. Scan size (a)–(c): 30×15 nm^2. Scan parameter: (a) V_S=0.5 V, I_T=50 pA, (b) V_S=1.0 V, I_T=50 pA, and (c) V_S=1.0 V, I_T=70 pA. (d) Coverage vs evaporation time. In the low coverage regime, a linear behavior is observed. The error bars of ± 0.01 atoms/nm^2 are estimated from different images and correspond to about $\pm 4-5$ atoms/450 nm^2.

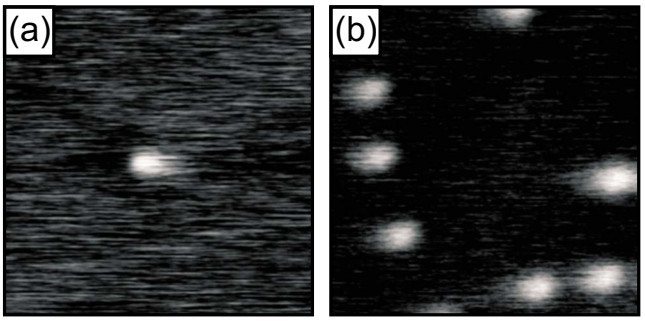

FIG. 4. (Color online) Constant frequency shift topographies of Au atoms adsorbed on alumina/NiAl(110). Scan size for (a) and (b): 9×9 nm^2. (a) Single Au atom surrounded by bare oxide; Δf=−350 mHz, V_S=−200 mV. (b) Ensemble of Au atoms at close spacing but separate; Δf=−900 mHz, V_S=−300 mV.

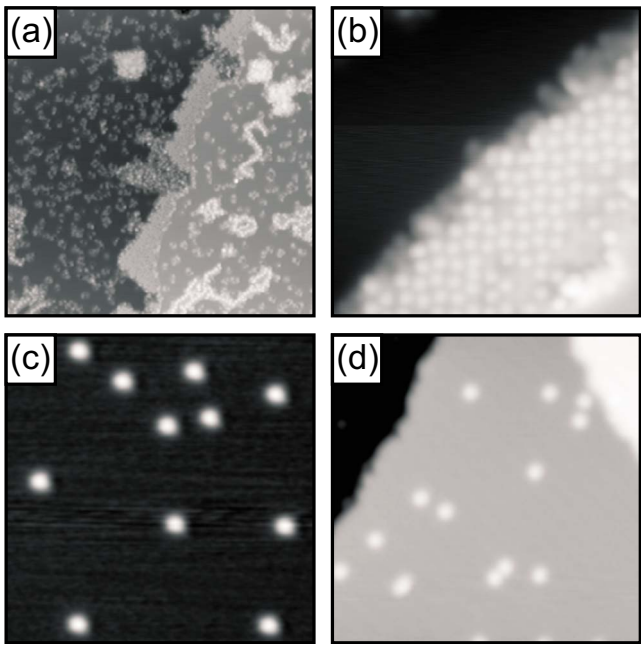

FIG. 5. (Color online) STM images of Li atoms on Ag(001).[(a) and (b)] Room temperature deposition by a SAES dispenser (Ref. 11). For highly dispersed adatom deposition [(c) and (d)] the microevaporator has been used in the low temperature environment. 0.02 ML of Li atoms deposited onto Ag(001). Scan parameters: (a) 80×80 nm^2, V_S=30 mV, I_T=25 pA; (b) 10×10 nm^2, V_S=30 mV, I_T=25 pA; (c) 18×18 nm^2, V_S=300 mV, I_T =50 pA; and (d) 18×18 nm^2, V_S=20 mV, I_T=25 pA.

advantage of a low temperature deposition for single adatom experiments becomes directly obvious from these images. Li deposited at room temperature prefers to aggregate and therefore Li-cluster are formed often located at steps but also on terraces. Furthermore, Li deposited at room temperature on Cu (Ref. 14) and NiAl (Ref. 15) can induce surface reconstructions since at room temperature the surface-Li interaction is stronger than at low temperature. The Li deposition at low temperature Figs. 5(c) and 5(d) shows highly dispersed single Li atoms perfect for single adatom experiments such as single atom contacts, single atom spectroscopy, or lateral manipulations. As a consequence, adatom deposition at low temperature is highly recommended for single adatom experiments.

IV. CONCLUSIONS

The presented STM and FM-DFM images prove that the proposed portable microevaporator enables the deposition of highly dispersed adsorbates onto a cold sample. Moreover, high coverages can be achieved. The simple construction ensures that it can be gripped by a manipulator and transported to the sample kept at low temperature in the STM/DFM stage. The heat transfer to the sample is negligible due to the small power used and the short evaporation time. Therefore, the surface analysis can be started directly after the deposition. The evaporated material is highly dispersed on the sample surface, prepared for all kinds of single adatom experiments. Very stable and reproducible deposition rates were obtained. In consequence, the results demonstrate adsorbate/sample conditions that are very well suited for manipulation experiments and studies of structure and nucleation. The wide application range of the microevaporator for dispersing different adsorbates onto a sample has been unambiguously shown.

ACKNOWLEDGMENTS

M.H. and M.N. would like to acknowledge the support of the Alexander von Humboldt Foundation. H.-J.F. acknowledges support from the Deutsche Forschungsgemeinschaft (DFG) through the Cluster of Excellence Unifying Concepts in Catalysis (UNICAT) as well as from the Donf der chemischen Industrie.

[1] F. Meier, L. Zhou, J. Wiebe, and R. Wiesendanger, Science **320**, 82 (2008).
[2] M. Ternes, C. P. Lutz, C. F. Hirjibehedin, F. J. Giessibl, and A. J. Heinrich, Science **319**, 1066 (2008).
[3] L. Bartels, G. Meyer, and K.-H. Rieder, Phys. Rev. Lett. **79**, 697 (1997).
[4] J. Repp, F. Moresco, G. Meyer, and K.-H. Rieder, Phys. Rev. Lett. **85**, 2981 (2000).
[5] L. Limot, J. Kröger, R. Berndt, A. Garcia-Lekue, and W. A. Hofer, Phys. Rev. Lett. **94**, 126102 (2005).
[6] D. M. Eigler and E. K. Schweizer, Nature (London) **344**, 524 (1990).
[7] N. Nilius, T. M. Wallis, and W. Ho, Science **297**, 1853 (2002).
[8] Y. Sugimoto, M. Abe, S. Hirayama, N. Oyabu, O. Custance, and S. Morita, Nature Mater. **4**, 156 (2005).
[9] M. Heyde, M. Kulawik, H.-P. Rust, and H.-J. Freund, Rev. Sci. Instrum. **75**, 2446 (2004).
[10] M. Heyde, G. H. Simon, H.-P. Rust, and H.-J. Freund, Appl. Phys. Lett. **89**, 263107 (2006).
[11] SAES Getters, Viale Italia 77, 20020 Lainate, Milan, Italy (2009).
[12] H.-P. Rust, M. Doering, J. I. Pascual, T. P. Pearl, and P. S. Weiss, Rev. Sci. Instrum. **72**, 4393 (2001).
[13] V. Simic-Milosevic, M. Heyde, N. Nilius, M. Nowicki, H. Rust, and H. Freund, Phys. Rev. B **75**, 195416 (2007).
[14] S. Mizuno, H. Tochihara, Y. Matsumoto, and K. Tanaka, Surf. Sci. **393**, L69 (1997).
[15] V. Saltas and C. Papageorgopoulos, Surf. Sci. **461**, 219 (2000).